THESIS FOR THE DEGREE OF LICENTIATE OF ENGINEERING IN THERMO AND FLUID DYNAMICS

Modeling of Spray Formation and Development in OpenFOAM with Application to Diesel and Alcohol Fuels

ANDREAS NYGREN

Department of Mechanics and Maritime Sciences
CHALMERS UNIVERSITY OF TECHNOLOGY

Göteborg, Sweden 2018

Modeling of Spray Formation and Development in OpenFOAM with Application to Diesel and Alcohol Fuels
ANDREAS NYGREN

Thesis for the degree of Licentiate of Engineering 2018:16
ISSN 1652-8565
Department of Mechanics and Maritime Sciences
Chalmers University of Technology
SE-412 96 Göteborg
Sweden
Telephone: +46 (0)31-772 1000

Chalmers Reproservice
Göteborg, Sweden 2018

Modeling of Spray Formation and Development in OpenFOAM with Application to Diesel and Alcohol Fuels
Thesis for the degree of Licentiate of Engineering in Thermo and Fluid Dynamics
ANDREAS NYGREN
Department of Mechanics and Maritime Sciences
Chalmers University of Technology

Abstract

Legislation with reagards to fuel emissions are becoming more stringent. This creates a need for improved engine concepts and fuels. This work is part of an ongoin project to create a concept for a direct injection dual fuel engine, which uses alcohol as main fuel and diesel as a pilot. The work in this thesis is part of the task to create a CFD model for this engine that can be used for improving the current engine concept.

The first part of this project has been to validate the in-house spray model, VSB2 for usage with alcohol fuels. This was done by comparing simululations made in OpenFOAM with experimental data obtained from the Chalmers HT/HP spray chamber. The simulations showed that the model could capture spray penetration at the simulation conditions accurately. It was also concluded that it was neccessary to fix the turbulent length scale in the injector cell to get an accurate prediction of the liquid penetration.

The second part of this project has been to improve upon the spray model. This has been done by extending the spray break up treament inside VSB2. The model was extended by implenting a mechanism for removing the stable droplets inside each blob and using these to create child parcels, containing only stable droplets. It was shown that this improves the prediction of liquid penetration, especially at lower temperatures.

The Third part of this project, that is still undergoing is to do CFD simulations of a direct injection dual fuel engine. Some preliminary results are shown in this work that show good agreement in the pressure trace. The sprays also ignites in a way that is expected, with the sprays closest to the pilot igniting first. There is still some uncertainty in the results, and further studies and development are needed to produce good results.

Keywords: Spray Formation, Spray Modeling, VSB2, Combustion

List of publications

This thesis is based on the work contained in the following publications:

Publication A A. Nygren and A. Karlsson, "Validation of the VSB2 Spray Model for Ethanol under Diesel like Conditions" in SAE Technical Paper 2017-01-2193, 2017.

Publication B A. Nygren and A. Karlsson, "A study of ECN Spray A using an Improved Stochastic Blob (VSB2) Spray Model" *To be presented at ICLASS 2018.*

The author of this thesis also contributed to the following publication:

Publication C T. Lackmann, A. Nygren, A. Karlsson and M. Oevermann, "Investigation of turbulence-chemistry interactions in a heavy-duty diesel engine with a representative interactive linear eddy model" *Accepted for publication in the International Journal of Engine Research.*

Acknowledgements

First and foremost I would like to acknowledge my supervisor Anders Karlsson for introducing me to the world of combustion CFD. It has been great to learn from you. Secondly, I would like to thank Ingemar Denbratt for hiring me and giving me the opportunity to work at the Division of Combustion and Propulsion systems.

I would also like to give special thanks to Harry Lehtiniemi for spending all these hours with me on Skype. I have really learned a lot from you.

Finally, I would like to thank my two colleauges Michael and Vignesh whom I share an office with. I was very lucky to start working here at the same time as you guys. Moving to Gothenburg would not have been half as fun if we all hadn't become friends so quickly.

The author gratefully acknowledges the finnacial support from the Swedish energy agency for this project.

Contents

1 Introduction

The process of combusting fuel and converting it into work in an engine as a mean of transportation has been the norm for the past century. However during the past decades, an increased awareness regarding the environmental and health impacts from the combustion products that arise from fossile fuels has increased significantly. The world is ever evolving, and with increased globalisation the need for transportation of goods and people will increase in the future. The European Commission investigated current trends in freight transportation, and projects that road freight traffic will increase by 57 % until 2050. [1]. Without any change, the increased need for transportation will lead to an increase in green house gas emissions (GHG), as well as an increase in other pollutants such as NO_x and particulate matter such as soot. This due to the fact that most of the worlds road bound transportation is done by heavy duty diesel trucks. These local emissions of NO_x and soot has been proven to be hazardous to humans [2], whereas green house gases such as CO_2 and CO has been proven to contribute to global warming, with 20 % of the total GHG in the EU coming from road transportation in 2015 [3]. Legislative responses to combat the increasing problems with emissions are becoming increasingly stringent.

1.1 Improved Engine Concepts and Fuels

To meet the futures demand for increased transportation as well as complying with increasingly stringent emission legislation, new engine technology and new fuels has to be developed. One of the issues with conventional diesel combustion has always been the NO_x-soot trade off. Soot tend to be crearted in areas that are fuel rich, which are formed due to the nature of the non-premixed combustion that occurs inside diesel engines [4]. Thus a richer mixture will typically lead to a larger formation of soot from diesel. A leaner mixture, closer to stoichiometric conditions will produce less soot, but also combust more efficiently leading to higher temperatures. Higher temperature promotes the oxidation of N_2 into NO and NO_2 through the Zeldovich mechanism [5].
New combustion concepts tries to address this by operating under conditions that promotes neither soot nor NO_x formation. These concepts include homogeneous charge combustion (HCCI), where the fuel is injected during the compression stroke. This early injection will cause the fuel to mix with the oxidizer before the combustion starts, leading to a lean mixture with negligible NO_x formation and no soot. However, HCCI has been shown to be difficult to control [6]. A promising extension of HCCI is the concept of reactivity controlled combustion (RCCI) [7]. This is a dual fuel concept, inch which two fuels are introduced into the cylinder. The two fuels consists of a low reactivity fuel that is introduced early during compression by port injection to create a premixed charge. The ignition is then controlled by introducing a high reactivity fuel directly into the cylinder. This allows for a greater control of the combustion compared to HCCI.
Another way of reducing emissions is to employ better fuels. Simple alcohol fuels, such as ethanol and methanol have been shown to produce negligible amount of soot compared to conventional petroleum based fuels [8]. Alcohol fuels also have a high combustion

efficiency due to the fact that the fuel molecule contain oxygen [9].

1.2 Direct Injection Dual Fuel Combustion

This thesis is part of a project to create an engine concept that utilizes direct injection dual fuel combustion. The concept consists of two fuels that are directly injected into the cylinder. First a pilot fuel with a high cetane number that can be ignited by compression ignition, then a main fuel with a high octane number that is in turn ignited by the pilot fuel. This allows for using a high octane number fuel such as ethanol or methanol as the main fuel in a compression ignited engine. Furthermore, using direct injection of both fuel give great controllability of the combustion phasing.

1.3 Objectives

The objective of this thesis is to support the development of the F-FLEX platform by numerical simulations. Computational fluid mechanics (CFD) can be used together with chemical reaction modeling and spray modeling to do time resolved 3D modeling of the mixing and combustion process inside an engine. This can give detailed information that is not obtainable by experiments. The first part of this project was to validate the in-house spray model VSB2 [10] for usage with alcohol fuels. The second part has been to improve the spray model, which has been done by implementing a new break up treatment, which is discussed further in chapter 3. This thesis mainly concerns the two first parts. The third part is to create a CFD model of the F-FLEX engine in the open-source CFD toolbox OpenFOAM [11], which can be used to improve upon the current engine concept as presented in [12]. This part is still undergoing, with some preliminary results included in this thesis.

2 Gas Phase Modeling

In this chapter the basics of the gas phase CFD modeling is introduced. This involves the discretization of several partial differential equations (PDE), which will all be introduced in this chapter. As this work revolves around a multi phase system, several of the equations will include source terms that represents the transfer of a quantity from the liquid phase to the gas phase.

2.1 Conservation of Mass and Momentum

The conservation of mass and momentum can be derived in differential form from first principles. The conservation of mass is expressed by the continuity equation:

$$\frac{\partial \rho}{\partial t} = \nabla(\rho \mathbf{u}) = \dot{S}_E \tag{2.1}$$

Where $\dot{S}_E$ is a time dependent source term, representing the evaporation of mass from the liquid phase to the gas phase. The conservation of momentum is expressed in the compressible Navier-Stokes equation:

$$\rho\left(\frac{\partial \mathbf{u}}{\partial t} + \mathbf{u}\cdot\nabla\mathbf{u}\right) = -\nabla p + \mu\nabla^2\mathbf{u} + \frac{1}{3}\mu\nabla(\nabla\cdot\mathbf{u}) + \rho g + \dot{S}_M \tag{2.2}$$

Where S_M is a source term that represents momentum transfer from the liquid phase to the gas phase. As eq (2.2) contain a non-linear convection term, solving it is not as straight forward as with a linear PDE. It requires an iterative procedure, such as the PISO [13] algorithm.

2.2 Energy Equation

Conversation of energy is a principle that derives from the first law of thermodynamics. In this work, total enthalpy is solved for as it can be considered a conserved quantity if changes in potential and kinetic energy is considered negligible. The conservation equation for total enthalpy is:

$$\frac{\partial \rho h}{\partial t} + \nabla(\rho \mathbf{u} h) = -\frac{Dp}{Dt} + \alpha\nabla^2 h + \dot{S}_h \tag{2.3}$$

Where $\dot{S}_h$ is a source term that represents the transfer of energy from the liquid phase to the gas phase due to heat transfer and heat of evaporation. The advantage of using total enthalpy instead of sensible enthalpy is that when chemical reactions occur, the total enthalpy is conserved, whereas the sensible enthalpy is not. Thus if sensible enthalpy would be used, another source term would be required.

2.3 Species Transport

The evolution of different species in time and space is governed by the species transport equation:

$$\frac{\partial \rho Y_i}{\partial t} + \nabla(\rho \mathbf{u} Y_i) = -\nabla^2 \mu_{\text{eff}} Y_i + \dot{\Omega}_i + \dot{S}_{i,E} \tag{2.4}$$

Where $\dot{\Omega}_i$ and $\dot{S}_{i,E}$ are source terms representing chemical reaction and evaporation of the liquid phase for specie i respectively.

2.4 Turbulence Modeling

Turbulence occurs in most fluid flow systems and are characterized by an increasingly chaotic flow as the Reynolds number increases. Eq (2.2) can account for this, but it requires that the smallest scales of turbulence known as the Kolmogorov scales are resolved in a simulation. This is known a a direct numerical simulation (DNS), and quickly becomes unfeasible at even moderate Reynolds numbers. More commonly, the Reynolds averaged Navier-Stokes (RANS) approach is used. This involves decomposing any quantity into it's mean value and a fluctuation from the mean value. Time averaging can then be applied to yield the Reynolds Averaged Navier-Stokes equation, which can then be solved to give the time averaged quantities. This procedure will give rise to another, unclosed term in eq (2.2):

$$R_{ij} = -\rho \overline{u_i' u_j'} \tag{2.5}$$

This term is commonly known as the Reynolds stress, and has to be modeled. In this work, the Reynolds stress is modeled using the $k - \varepsilon$ model [14], which assumes isotropic turbulence. k is referred to as turbulent kinetic energy and ε is referred to as turbulent dissipation. The transport equations for k and ε are given by:

$$\frac{\partial \rho k}{\partial t} + \nabla(\rho u \varepsilon) = \nabla \left[\left(\frac{\mu_t}{\sigma_k} + \mu \right) \nabla k \right] + \mu_t \left[S - \frac{2}{3}(\nabla u)^2 \right] - \frac{2}{3}\rho k \nabla u - \rho \varepsilon \tag{2.6}$$

$$\frac{\partial \rho \varepsilon}{\partial t} + \nabla(\rho \varepsilon u) = \nabla \left[\left(\frac{\mu_t}{\sigma_\varepsilon} + \mu \right) \nabla \varepsilon \right] + \mu_t C_1 \frac{\varepsilon}{k} \left[S - \frac{2}{3}(\nabla u)^2 \right] - \frac{2}{3} C_1 \rho \varepsilon \nabla u - C_2 \rho \frac{\varepsilon^2}{k} + C_3 \rho \varepsilon \nabla u \tag{2.7}$$

Where:

$$S = 2 S_{ij} S_{ij} = \frac{1}{2} \left(\frac{\partial u_j}{\partial x_i} + \frac{\partial u_i}{\partial x_j} \right)^2 \tag{2.8}$$

A well known drawback of the $k - \varepsilon$ model is its inability to predict the spreading of a round jet. One way to better account for that is to tune the constants in the model. The tuning constants in this work can be found in table 2.1.

Table 2.1: Constants used with the $k - \varepsilon$ model

C_1	C_2	C_3	C_μ	σ_k	σ_ε
1.55	1.92	-0.33	0.09	1.0	1.53

2.5 Combustion Modeling

The reaction source term $\dot{\Omega}_i$ in equation 2.4 arises when chemical reactions need to be taken into account. One such case would be when combustion occurs. For the engine simulations in this work the well stirred reactor approach was used to calculated the reaction source term. In this approach every cell is considered as a closed homogeneous reactor. The chemistry can then be solved separately over the time step in each as a system of ordinary differential equations. A linearized source term can then be constructed based on the new species mass fraction:

$$\dot{\Omega}_i = \frac{\rho(Y_{i,1} - Y_{i,0})}{\Delta t} \tag{2.9}$$

The advantage of this approach is that it is easy to implement, straight forward to use and incorporates the effects of finite rate chemistry. The disadvantage is that it does not take turbulence-chemistry interactions into account, leading to an faster rate of heat release and increased maximum temperature. Also, if a detailed chemical mechanism is used, this approach can be computationally intensive as a large system of ordinary differential equations have to be solved in each cell. In this work, the LOGESoft chemistry solver was used for all chemistry calculations. It utilizes cell clustering to speed up chemistry integration by clustering cells together based on some variable and solving those cells together.

3 Spray Formation and Modeling

In this chapter an introduction to spray formation and modeling will be given. In addition, a detailed description of the VSB2 spray model will be given.
The typical way of modeling sprays in CFD is to use the Eulerian-Lagrangian approach. Where the continuous phase is modeled in a Eulerian frame of reference (as described in chapter 2), and the dispersed phase is modeled in a Lagrangian frame of reference.

3.1 Spray Formation

When a liquid is injected at a high velocity relative its surroundings a jet will form and start to break up. This is commonly referred to as primary break up, and the mechanisms by which this occurs depends on the regime of the break up. For primary break up, four different regimes are usually identified depending on the Ohnsorge and liquid Weber numbers [15]. These are the Rayleigh regime, the first and second wind regimes and the atomization regime. For high pressure injection inside of a diesel engine, the atomization regime is the most relevant one.
In the atomization regime, primary break up occurs almost imminently which causes the liquid jet to split up into ligaments and a small conical liquid core is typically formed near the nozzle. Due to the large drag forces create by the high relative velocity, the spray will break up further into small droplets. This is refereed to as secondary break up. Several regimes can be identified for the secondary break up based on the gas phase Weber number:

$$We_g = \frac{\rho_g u_{\text{rel}}^2 d}{\sigma} \tag{3.1}$$

The Weber number describes the ratio of the drag force to the surface tension of a droplet. The surface tension is what is holding the droplet together, and if the drag force is large enough relative to the surface tension, a droplet will tend to break up into smaller more stable droplets. Depending on the author, several regimes can be identified in literature for secondary break up. However, the main regimes are vibrational break up, bag break up, stripping break up and catastrophic break up [15]. All of these regimes are relevant inside an engine, and they occur with an increased magnitude of the Weber number. Further away from the injector, small droplets will have formed du to the above mentioned processes. These small droplets are then evaporated easily due to the high ambient temperature, and the fuel can then be ignited. Thus accurate prediction of the spray formation is important to predict when and where the fuel ignites.

3.2 Spray Modeling

As previously mentioned, the most common way to model sprays in CFD is to use the Eulerian-Lagrangian approach. In this approach, point parcels represents a collection of real droplets that are evolved with the flow over time using Newtonian mechanics. The coupling between gas and liquid phase as well as the impact of spray break up is

governed by sub models. For sprays that are operating in the atomization regime, it is common to not use any sub model for primary break up, but instead use the so called blob injection method [16]. In this method, spherical blobs (which represents actual droplets) are injected into the domain with a diameter of that of the injector nozzle. Thus forming a large collection of bigger blobs in the nozzle area, which mimics the near nozzle liquid core that is observed in the atomization regime. These blobs are then broken up by the flow.
The secondary break up is then typically modeled by a sub model. Commonly used models for secondary break up include the TAB model and the Kelvin-Helmholtz Rayleigh-Taylor model. A problem with many of these models are that they contain an excessive amount of tuning parameters that need to be set. In this work the VSB2 model has been used, which will be described further in the next section.

3.3 The VSB2 Spray Model

3.3.1 Model Overview

The Stochastic Blob and Bubble model (VSB2) is a Eulerian-Lagrangian spray model. It was designed to be unconditionally robust, with a minimal amount of tuning parameters and to be able to implement in any CFD code that supports particle tracking. It has previously been successfully implemented in the commercial CFD code STAR-CD [17] and the open source code OpenFOAM 1.6.x. [10, 18] In this work the VSB2 model has been migrated to OpenFOAM 2.2.x.

3.3.2 Blob and Bubble Approach

The main difference between VSB2 and more traditional Lagrangian spray models is how the computational parcel is defined. The common way of doing it is to have one parcel represent a collection of equally sized actual droplets. In the VSB2 model the computational parcels are referred to as blobs, and contain collection of different droplet sizes.
The model also feature the inclusion of a bubble, that limits the volume inside each grid cell that the blob can interact with. The diameter of the bubble is given by:

$$D_{bub} = D_B + l_t \tag{3.2}$$

Where D_B is the blob diameter and l_t is the turbulent length scale given by:

$$l_t = C_\mu^{\frac{3}{4}} \frac{k^{\frac{3}{2}}}{\varepsilon} \tag{3.3}$$

The volume of the bubble is then given by:

$$V_{bub} = N_D \frac{\pi}{6}[(D_B + l_t)^3 - D_B^3] \tag{3.4}$$

If the bubble volume is larger than the cell volume ($V_{bub} > V_{cell}$), then the blob will interact with the cells volume. A schematic overview of the difference between VSB2 and traditional spray models can be seen in figure 3.1.

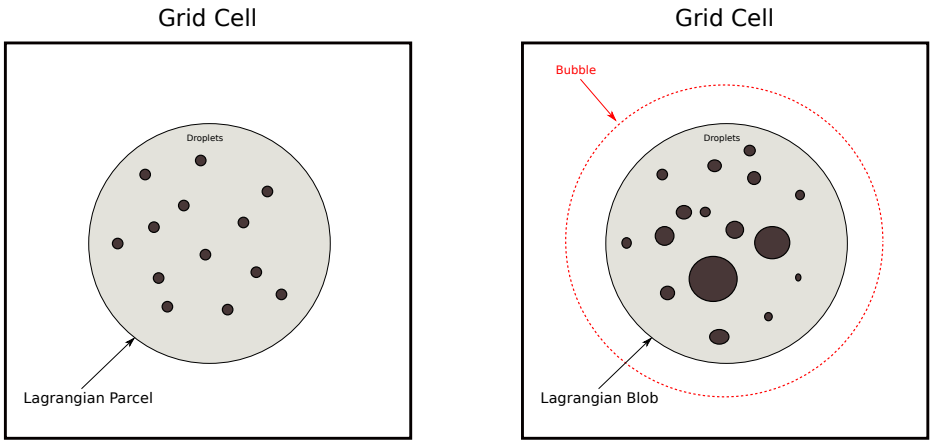

(a) *Traditional spray model* (b) *VSB2*

Figure 3.1: *Comparison of VSB2 to traditional spray models*

3.3.3 Secondary Break up in VSB2

As mentioned previously, the main difference between VSB2 and traditional spray models is that in VSB2 each blob represents a collection of different droplet sizes. The distribution of the droplet sizes inside each blob is governed by a one parameter distribution function. Depending on the conditions that the blob is experiencing, the distribution function will have a different shape. Thus the impact of secondary break up on the droplet sizes is modeled through the shape of the distribution function inside each blob. An overview on how the distribution function is constructed will be given in this section. Further details can be found in [10].
The new blob diameter that is formed by secondary break up is given by:

$$D_1 = D_s + (D_0 - D_s) \cdot e^{\frac{-\Delta t}{\tau_{\text{breakup}}}} \tag{3.5}$$

Where τ_{breakup} is a dimensionless droplet break up time scale which depends on the current break up regime. In VSB2 this is calculated from the Pilch-Erdman correlation [19]. D_0 is the current blob diameter, and D_s is the stable droplet diameter under these conditions which is given by:

$$D_s = \frac{We_{\text{cr}}\sigma}{\rho_{\text{gas}} U_{\text{rel}}^2} \tag{3.6}$$

The critical Weber number is correlated with the Ohnesorge number:

$$We_{\text{cr}} = 12(1 + 1.0077\ Oh^{1.6}) \tag{3.7}$$

Using these quantities a power-law distribution function of the droplet sizes inside each blob can be defined:

$$D = M^f \tag{3.8}$$

Where D, is the droplet diameter normalized by D_0 and M is normalized mass. The power law coefficient, f is then defined by:

$$f = \frac{\log\left(\frac{D_s}{D_0}\right)}{\log\left(1 - \left(\frac{D_1}{D_0}\right)\right)} \tag{3.9}$$

This procedure is done for each blob in the system. Thus each blobs will have a different shape of its distribution function, depending on what type of break up it is currently undergoing.
The blob is then divided into ten mass intervals, where the first interval contains the stripped off mass. The remaining mass is then divided equally into the remaining nine intervals. Using the distribution function, these intervals produce ten different droplet size intervals. In each droplet size interval, one droplet size is sampled randomly. These sampled droplets are then chosen to interact with the gas mass, and their contribution is summed up for each blob.

3.3.4 Gas Phase Coupling

As explained in chapter 2, the coupling from the liquid phase to the gas phase is done through source terms. In the VSB2 model, the gas-phase coupling is done by first calculating the equilibrium state between the gas and the liquid in each cell. This makes the model very robust, as the mass and energy transfer cannot exceed that of the equilibrium state. The equilibrium state is determined for each blob by evaporating a small amount of mass until saturation is reached. When the equilibrium mass and temperature has been determined, relaxation equations are applied to both quantities based on a relevant time scale. This will yield actual transfer of mass and energy to the gas phase. The relaxation equations for mass and temperature are:

$$\frac{dm_{blob,i}}{dt} = \frac{m_{eq,i} - m_{blob,i}}{\tau_m} \tag{3.10}$$

$$\frac{dT_{blob,i}}{dt} = \frac{T_{eq,i} - T_{blob,i}}{\tau_T} \tag{3.11}$$

Here, the index i denotes the droplet size interval inside a blob. The contribution for each size interval is summed up for each blob. The relevant time scales are correlated by dimensionless numbers in the following way:

$$\tau_m = \frac{\rho_{blob} D_{blob,i}^2 R T_m}{6pDSh} \tag{3.12}$$

$$\tau_T = \frac{\rho_{blob} D_{blob,i}^2 C_{p,blob}}{6\lambda f(z) Nu} \tag{3.13}$$

Where Sh is the Sherwood number and Nu is the Nusselt number. $f(z)$ is a correction factor that accounts for the reduction in heat transfer due to strong evaporation [20]. These time scales are commonly employed in traditional spray models.

For the momentum transfer, the standard drag coefficient approach is used. The drag coefficient is correlated based on the Reynolds an Weber number to also account for droplet deformation:

$$C_d = 0.28 + \frac{21}{Re} + \frac{6}{\sqrt{Re}} + We(0.2319 - 0.1579\log(Re) + 0.0471\log^2(Re) - 0.0042\log^3(Re)) \tag{3.14}$$

The relaxation time scale for momentum is given by:

$$\tau_U = \frac{4\rho_{blob} D_{blob,i}}{3\rho_g C_d U_{rel}} \tag{3.15}$$

The droplet velocity can then be updated according to:

$$U_{blob,i} = \frac{U_{blob} + U_g \frac{\Delta t}{\tau_U}}{1 + \frac{\Delta t}{\tau_U}} \tag{3.16}$$

The updated droplet velocities can be used together with the updated droplet masses to give the contribution of momentum for the entire blob.

3.3.5 Improving the break up treatment in VSB2

The VSB2 model accounts momentum transfer by summing up the contribution for all droplets sizes to the blob. A downside with this approach is that the smaller stable droplets contained in the blob will travel with the same momentum as the larger unstable droplets inside the same blob. Thus they will continue to travel downstream even though, in reality they are much smaller and should have far less momentum and lower relative velocity than the larger unstable droplets inside the blob. To improve upon this, the break up treatment has been modified to remove the stable droplets from the blob and create a "child blob", containing only droplets that are stable under the circumstances. The procedure is illustrated in figure 3.2.

3.3.6 Fixing the Turbulent Length Scale.

The VSB2 model feature the ability to fix the turbulent length scale inside the injector to act as a boundary condition inside that cell during the injection. This is done by fixing ε inside the cell according to a turbulent length scale:

$$\varepsilon_{inj} = C_\mu^{3/4} \frac{k^{3/2}}{l_t} \tag{3.17}$$

Where the turbulent length scale is typically taken to be 10 % of the nozzle diameter:

$$l_t = 0.1 \cdot d_{\text{nozzle}} \tag{3.18}$$

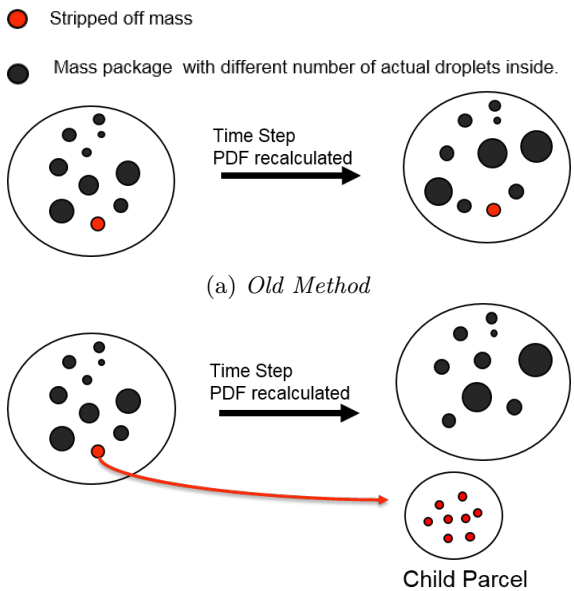

(a) *Old Method*

(b) *New Method*

Figure 3.2: *Schematic comparison illustrating the difference between the new and old break up treatment.*

4 Case Summary

In this chapter, different cases that has been used in this work will be presented.

4.1 Chalmers HT/HP Spray with Ethanol

Data from the Chalmers high temperature/high pressure spray chamber was used for validating the VSB2 spray model for ethanol. A detailed explanation of the experimental setup can be found in [21].

4.2 ECN Spray A

Data from the engine combustion network(ECN) [22] was used to validate the improved break up treatment. The ECN spray A refers to n-dodecane spray at diesel engine like conditions. Data is available for a range of ambient conditions. The data that was used in this work is summarized in table

	Ambient Temperature	Ambient Pressure	Gas density
Case A	900 K	60.5 Bar	22.9 kg/m^3
Case B	700 K	46 Bar	22.9 kg/m^3

4.3 Direct Injection Dual Fuel Engine

The Direct Injection Dual Fuel Engine refers to a direct injection dual fuel engine, with a centrally placed main injector and an asymmetrically placed pilot injector. As an initial test, one of the engines mid-load points was simulated. Methanol was used as main fuel and n-dodecane was used as diesel surrogate for the pilot fuel. The methanol is injected from an injector with an eight hole nozzle, whereas the pilot fuel is injected from an injector with a three hole nozzle. The engine grid that was used is shown in figure 4.1. To account for piston motion, a mesh layering technique was used that is included in LibICE, developed at Politecnico di Milano [23]. A chemical mechanism containing 386 species and 2331 [24] reactions was used for calculating the chemical source term. The engine load point and injection timings are summarized in table 4.1. The experimental data was obtained from a single cylinder heavy duty engine. A more detailed description of the real engine setup and operation can be found in [12].

Table 4.1: Engine load and Injection timings of the F-FLEX baseline case

Engine Speed [RPM]	1262
Engine Load [Nm]	172
SOI_{pilot} [CAD bTDC]	14.16
EOI_{pilot} [CAD bTDC]	11.04
SOI_{main} [CAD bTDC]	4.10
EOI_{main} [CAD aTDC]	7.28

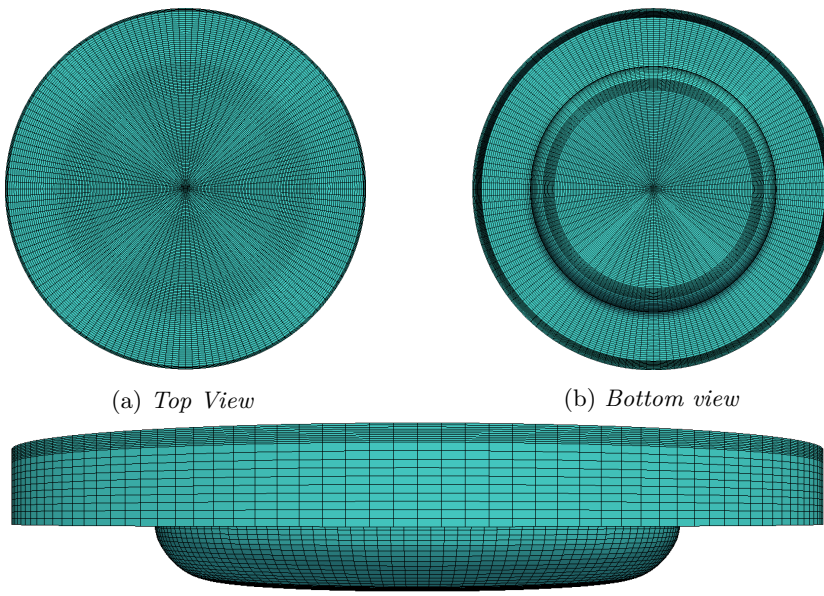

(a) *Top View* (b) *Bottom view*

(c) *Side view*

Figure 4.1: *Mesh of the F-FLEX piston geometry used in the engine computations.*

5 Engine Results

In this chapter a summary of one preliminary result from simulating the direct injection dual fuel engine.
Figure 5.1 show the simulated pressure trace compared to experimental data. It show that the simulation matches the experiments quite well. A slightly higher increase in cylinder pressure can be observed compared to the experimental data. However a faster combustion is expected when using the well stirred reactor approach, as the turbulence chemistry interaction is not modeled.
Figure 5.2 show an iso-surface of the stoichiometric mixture fraction for methanol ($Z_{st} = 0.13$), colored by temperature at different times. It can be seen that two sprays are ignited first, and the rest are ignited slightly later. The first sprays that are ignited are the ones that are closes to the pilot. However, there is no indication that there is any problems igniting the rest of the sprays. It should be noted that these results are preliminary, and some more work is needed to ensure robustness of the simulations.

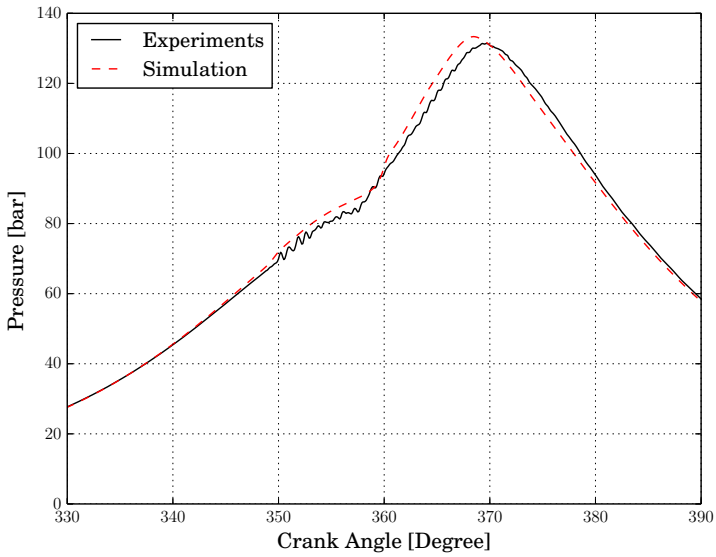

Figure 5.1: *Simulated and experimental pressure trace for the FFLEX engine at mid load.*

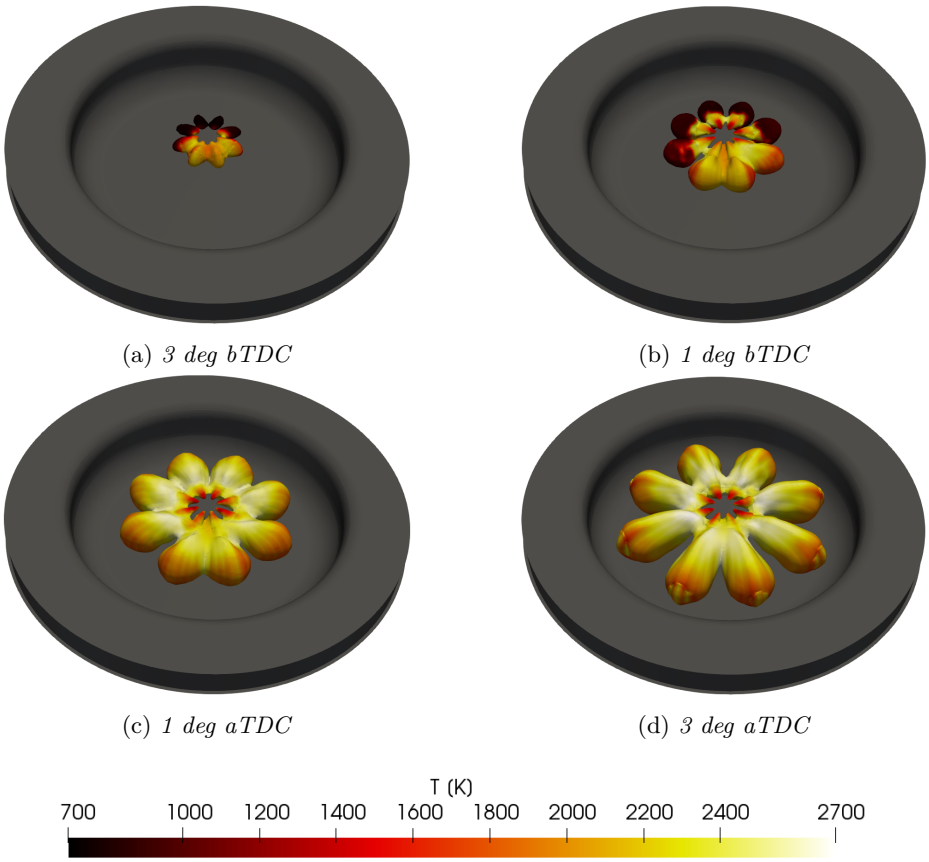

(a) *3 deg bTDC*

(b) *1 deg bTDC*

(c) *1 deg aTDC*

(d) *3 deg aTDC*

Figure 5.2: *Isosurface made at stoichiometric mixture fraction of methanol. Colored by temperature*

6 Contribution to the Field

6.1 Paper I

"Validation of the VSB2 Spray Model for Ethanol under Diesel like Conditions"

The first required step for this thesis was to validate the in house spray model, VSB2 for use with alcohol fuels. Ethanol was chosen for this validation, as ethanol spray experiments were performed in parallel inside the project. A study was done on the ethanol spray, where different turbulence models were tested and the impact of fixing the turbulent length scale in the injector cell was also investigated. It could be shown that with tuning, the VSB2 model could accurately predict spray penetration for the conditions that were investigated. It was also concluded that it was necessary to fix the turbulent length scale in the injector cell.

6.2 Paper II

"A Study of ECN Spray A Using an Improved Stochastic Blob (VSB2 Spray Model)"

In this paper, the break up treatment of the VSB2 model was extended to create child parcels from the stable droplets. The extension was successfully implemented in the current version of the model. The model was tested for different parametric variations of ECN Spray A. It was shown that using the new break up treatment, gave a better prediction of the liquid penetration with the effect being more pronounced at lower temperature. The effect was credited to the fact that if the smaller stable droplets are contained in separate blobs, these blobs will be more easily dispersed to the bulk flow where more energy is available for evaporation. Radial profiles of the fuel vapor concentration supports this reasoning, showing that the gas becomes more radially dispersed when using the new break up method.

6.3 Paper III

"Investigation of turbulence-chemistry interactions in a heavy-duty diesel engine with a representative interactive linear eddy model"

.In this paper, a representative interactive linear eddy model (RILEM) [25] is compared with the well stirred reactor approach for a heavy duty Volvo engine case. The author of this thesis contributed to this work by supplying the engine cases and performing the well stirred reactor simulations that was used to compare with the RILEM model.

7 Conclusion & Future work

The objective of validating and improving upon the VSB2 spray model has been presented in this thesis. The results from publication A show that the VSB2 model can predict the spray penetration of ethanol without any inherent modifications to the model. Furthermore, publication B show promising results with regards to improving the break up treatment in VSB2. Especially in the low temperature cases. This approach could be further improved by creating child blobs based on all droplet size interval instead of just the stable droplets. The next step is to finalize the CFD model for the F-FLEX engine and validating it against experimental data. This model can then be used to investigate parameters that are more difficult to change in an experimental setup, such as injector configuration and piston geometries. It is also of interest to investigate high load points that are difficult to test experimentally due to safety concerns. Further along in the project, it could be of interest to explore more advanced combustion models. As mentioned in chapter 2, the well stirred reactor approach does not account for turbulence-chemistry interaction. Not accounting for this will leads to mode rapid combustion and higher temperatures. This in turn will lead to an over-prediction of pollutants such as NO_x.

References

[1] European Commission, 2016. *EU, Reference Scenario 2016: Energy, Transport and GBG Emission Trends to 2050*.

[2] H.E. Institute , 1995. *Diesel Exhaust: A critical analysis of Emissions, Exposure and Health Effects*.

[3] European Environment Agency, 2017. *Key trends and drivers in greenhouse gas emissions in the EU in 2015 and over the past 25 years*.

[4] J. E. Dec, "A Conceptual Model of DI Diesel Combustion Based on Laser-Sheet Imaging," 1997. SAE Technical Paper 970873.

[5] J. Zeldovich, "The oxidation of nitrogen in combustion and explosions,"

[6] D. Blom, M. Karlsson, K. Ekholm, P. Tunestål, and J. R., "HCCI engine modeling and control using conservation principles," 2008. SAE Technical Paper 2008-01-0789.

[7] R. D. Reitz and G. Duraisamy, "Review of high efficiency and clean reactivity controlled compression ignition (RCCI) combustion in internal combustion engines," *Progress in Energy and Combustion Science*, vol. 46, pp. 12–71, 2014.

[8] C. S. McEnally and L. D. Pfefferle, "Sooting tendencies of oxygenated hydrocarbons in laboratory-scale flames," *Environmental Science and Technology*, vol. 45, no. 6, pp. 2498–2503, 2011.

[9] V. R. Surisetty, A. K. Dalai, and J. Kozinski, "Alcohols as alternative fuels: An overview," *Applied Catalysis A: General*, vol. 404, no. 1-2, pp. 1–11, 2011.

[10] A. Kösters and A. Karlsson, "VALIDATION OF THE VSB2 SPRAY MODEL AGAINST SPRAY A AND SPRAY H," *Atomization and Sprays*, vol. 26, no. 8, pp. 775–798, 2016.

[11] H. G. Weller, G. Tabor, H. Jasak, and C. Fureby, "A tensorial approach to computational continuum mechanics using object-oriented techniques," *Computers in Physics*, vol. 12, no. 6, p. 620, 1998.

[12] M. Saccullo, T. Benham, and I. Denbratt, "Dual Fuel Methanol and Diesel Direct Injection HD Single Cylinder Engine Tests," 2018. SAE Technical Paper 2018-01-0259.

[13] R. I. Issa, "Solution of the implicitly discretised fluid flow equations by operator-splitting," *Journal of Computational Physics*, vol. 62, no. 1, pp. 40–65, 1986.

[14] B. Launder and D. Spalding, "The numerical computation of turbulent flows," *Computer Methods in Applied Mechanics and Engineering*, vol. 3, no. 2, pp. 269–289, 1974.

[15] C. Baumgarten, *Mixture Formation in Internal Combustion Engines*. Springer-Verlag, 2006.

[16] R. Reitz and R. Diwakar, "Structure of High-Pressure Fuel Sprays," *SAE Paper 870598*, 1987.

[17] T. Husberg, I. Denbratt, and A. Karlsson, "Analysis of Advanced Multiple Injection Strategies in a Heavy-Duty Diesel Engine Using Optical Measurements and CFD-Simulations ," *SAE Technical Paper 2008-01-1328*, 2008.

[18] A. Kösters and A. Karlsson, "Modeling of Diesel Fuel Spray Formation in OpenFOAM," 2011. SAE Technical Paper 2011-01-0842.

[19] M. Pilch and C. Erdman, "Use of breakup time data and velocity history data to predict the maximum size of stable fragments for acceleration-induced breakup of a liquid drop," *International Journal of Multiphase Flow*, vol. 13, no. 6, pp. 741–757, 1987.

[20] M. El Wakil, O. Ueyhara, and F. Myers, "A Theoretical Investigation of Heating-up Period of Injected Fuel Droplets Vaporizing in Air.," 1954. NACA Report No. TN3179.

[21] M. Saccullo, M. Andersson, J. Eismark, and I. Denbratt, "High Pressure Ethanol Injection under Diesel-Like Conditions," 2017. SAE Technical Paper 2012-01-1263.

[22] Engine Combustion Network, 2018. https://ecn.sandia.gov/.

[23] Lucchini, T. and D'Errico, G. and Jasak, H. and Tukovic, Z., "Automatic Mesh Motion with Topological Changes for Engine Simulation," 2007. SAE Technical Paper 2007-01-0170.

[24] A. Borg and H. Lehtiniemi, "Fuel flexible engine platform reaction scheme." LOGE AB, Confidential Report, October 2017.

[25] T. Lackmann, A. R. Kerstein, and M. Oevermann, "A representative linear eddy model for simulating spray combustion in engines (RILEM)," *Combustion and Flame*, vol. 193, pp. 1–15, 2018.